Front. Electr. Electron. Eng. China 2008, 3(1): 61–69
DOI 10.1007/s11460-008-0022-6

RESEARCH ARTICLE

Yuanxin WANG, Wensheng FAN, Weiyan PAN, Hongqi ZHANG

Spherical harmonic series solution of fields excited by vertical electric dipole in earth-ionosphere cavity

Abstract The spherical harmonic series expression of electromagnetic fields excited by ELF/SLF vertical electric dipole in the spherical earth-ionosphere cavity is derived when the earth and ionosphere are regarded as non-ideal conductors. A method of speeding numerical convergence has been presented. The electromagnetic fields in the cavity are calculated by this algorithm, and the results show that the electromagnetic fields between the earth and the ionosphere are the sum of two traveling waves in the SLF band. Moreover, the results are in complete agreement with that of the well-known spherical second-order approximation in the SLF band. The electromagnetic fields in the cavity are a type of standing wave in the ELF band and the variation of the amplitude versus frequency coincides with Schumann's resonance.

Keywords spherical harmonic series, speeding numerical convergence, Schumann's resonance

1 Introduction

According to the ITU's definition of the frequency spectrum in the low frequency band, 3–30 kHz is called VLF, 300 Hz–3 kHz is known as ULF, 30–300 Hz is considered SLF and frequency spectra below 30 Hz are called ELF. The ground and the ionosphere are both good reflecting surfaces for electromagnetic waves with frequencies of less than 30 kHz, and the wave actually propagates in spherical earth-ionosphere guide, so it is generally defined as earth-ionosphere guide [1]. To meet the requirements of communication and develop navigation systems, the radiowave propagation theory of the VLF and SLF [2] band has been in development since the 1960s-1970s. In the VLF band, the electromagnetic field of the wave guide is taken as the sum of a number of "wave modes", each of which has its own phase speed and attenuation rate, whose height-gain functions are "orthogonal" to each other. In the SLF band, for example, as for $f = 100$ Hz, there is only one TEM waveguide mode which may be propagated in the wave guide, while the others are the rapid attenuation wave modes. Each wave mode of the VLF and SLF bands is generally solved from the "modal equation", whose theoretical calculation has already been verified by numerous experiments in the VLF and SLF frequency band [3].

Earthquake prediction researchers have discovered that just before an earthquake occurs, low-frequency electromagnetic radiation often appears [4]. The frequency spectrum of this type of radiation is very wide, but the primary energy concentrates in the SLF and ELF band. To further explore this phenomenon and attempt to uncover the rule of earthquake electromagnetic radiation as an indicator of earthquake occurrence, it is imperative that the electric wave propagation rules along the ground in the SLF low end and ELF frequency bands be studied. In SLF low end and ELF band, for example, as for an electric wave of $f = 10$ Hz, its wavelength is equal to 30000 kilometers. In this situation, the propagation space between the ground and the ionosphere cannot be regarded as a "wave guide", but as a "shell". Thus, VLF/SLF wave propagation [5] theory cannot be applied again to the ELF band.

The solution to the electromagnetic field question in the spherical coordinate system consists of many methods [6,7]. In 1999 Donald E. Barrick [8] proposed a kind of spherical harmonic series algorithm of ELF vertical electric dipole in earth-ionosphere shell, which was able to obtain the solution to the electromagnetic

Translated from *Chinese Journal of Radio Science*, 2007, 22(2): 204–211 [译自: 电波科学学报]

Yuanxin WANG (✉), Weiyan PAN, Hongqi ZHANG
Qingdao Branch, Chinese Research Institute of Radiowave Propagation, Qingdao 266071, China
E-mail: wyx781215@163.net

Wensheng FAN
The Communication Department of Chinese Navy Headquarters, Beijing 100841, China

fields question when the ground and ionosphere were both ideal conductors. However, the author did not attain the same results under conditions when both the ground and the ionosphere were non-ideal conductors. Besides this, the variations of the electromagnetic field along the height and in relation to the frequency in the shell were not explored further. In this paper we will first derive the spherical harmonic series expressions of electromagnetic fields in the shell under conditions when both the Earth and ionosphere are non-ideal conductors. We also propose a kind of speeding numerical convergence algorithm, based on which the variations of the electromagnetic field along the ground and the height, as well as the variations of the frequency within the shell, are analyzed and calculated. Independent verification will show that our findings completely coincide with the known correct theoretical calculation result.

2 Spherical harmonic series expansion of fields in earth-ionosphere guide

From spherical coordinates shown in Fig. 1, the ground and the ionosphere are an ideal reflection wall with certain surface impedance. They are separately recorded as Δ_g and Δ_i. Their distances from the center are r_a (6370 km) and $r_c = r_a + h$ respectively. h is the height of ionosphere from earth. Excitation source is idealized as a vertical electric dipole, whose current moment is $I\mathrm{d}l$ which is placed in the position of $r = r_b$, $\theta = 0^\circ$ (z direction).

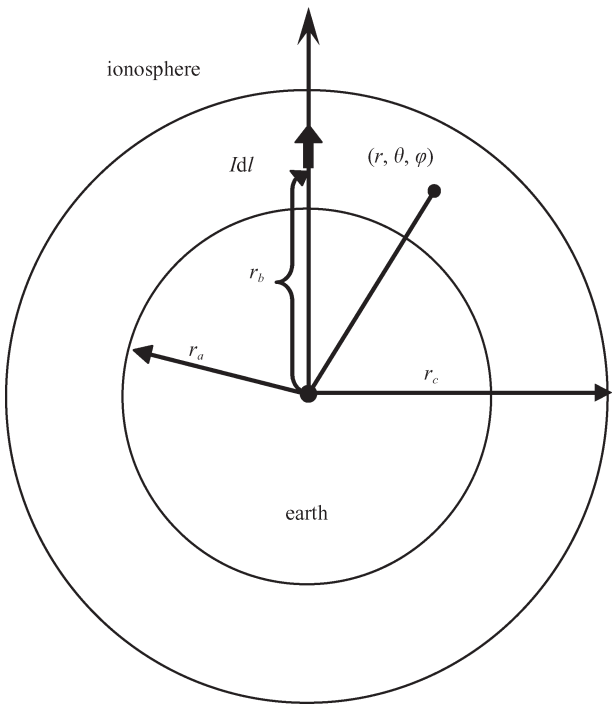

Fig. 1 Earth-ionosphere guide

The electromagnetic field of wave guide may be expressed by a potential function (Debye potentials),

$$E_r = \frac{1}{-\mathrm{i}\omega\varepsilon}\left(\frac{\partial^2}{\partial r^2} + k^2\right)U, \tag{1}$$

$$E_\theta = \frac{1}{-\mathrm{i}\omega\varepsilon r}\frac{\partial^2 U}{\partial r \partial\theta}, \tag{2}$$

$$H_\varphi = \frac{-1}{r}\frac{\partial U}{\partial\theta}, \tag{3}$$

where potential function U should satisfy the differential equation as below:

$$\left(\nabla^2 + k^2\right)\frac{U}{r} = 0. \tag{4}$$

When it is excited by the vertical electric dipole and the ground and the ionosphere do not exist, the potential function of the primary field excited by the vertical electric dipole in the position of $r = r_b$, $\theta = 0^\circ$ can be expressed as:

$$U_0^{\mathrm{VED}} = \frac{ikI\mathrm{d}l}{4\pi v_b^2}T_0, \tag{5}$$

where,

$$T_0 = \begin{cases} \sum\limits_{n=0}^{\infty}(2n+1)H_n(v_\mathrm{b})j_n(v)P_n(\cos\theta),\ v < v_b \\ \sum\limits_{n=0}^{\infty}(2n+1)j_n(v_\mathrm{b})H_n(v)P_n(\cos\theta),\ v > v_b \end{cases}, \tag{6}$$

and

$$v_b = kr_b, v = kr. \tag{7}$$

$P_n(\cos\theta)$ is the first kind of Legendre function, $j_n(v)$ is the first kind of half integer order Bessel function $\sqrt{\pi v/2}J_{\mathrm{n}+1/2}(v)$, $H_\mathrm{n}(v)$ is the first kind of half integer order Hankel function $\sqrt{\pi v/2}H^{(1)}_{\mathrm{n}+1/2}(v)$. They satisfy the differential equation:

$$\left(\frac{\mathrm{d}^2}{\mathrm{d}v^2} + 1\frac{n(n+1)}{v^2}\right)B_n(v) = 0. \tag{8}$$

When the vertical electric dipole is located between the ground and the ionosphere, due to the reflection of the ground and the ionosphere, the secondary disturbance field in the wave guide will be produced, and its general expression can also be expanded according to the spherical harmonic function. It may be

rewritten as:

$$U_s^{\mathrm{VED}} = \frac{\mathrm{i}kI\mathrm{d}l}{4\pi v_b^2}\sum_{n=0}^{\infty}(2n+1)[b_n j_n(v)+c_n H_n(v)]P_n(\cos\theta). \tag{9}$$

The total field in the wave guide should be expressed as:

$$U^{\mathrm{VED}} = U_0^{\mathrm{VED}} + U_s^{\mathrm{VED}} = \frac{\mathrm{i}kI\mathrm{d}l}{4\pi v_b^2}\begin{cases}\sum\limits_{n=0}^{\infty}(2n+1)[c_n H_n(v)+(H_n(v_b)+b_n)j_n(v)]P_n(\cos\theta), & v<v_b\\ \sum\limits_{n=0}^{\infty}(2n+1)[b_n j_n(v)+H_n(v)(c_n+j_n(v_b))]P_n(\cos\theta), & v>v_b\end{cases}. \tag{10}$$

In the surface of $r = r_a$, the electromagnetic field should satisfy the ground impedance boundary condition, which is expressed as:

$$\left.\begin{aligned}E_\theta &= -\Delta_{\mathrm{g}} Z_0 H_\varphi\\ E_\varphi &= \Delta_{\mathrm{g}} Z_0 H_\theta\end{aligned}\right|_{r=r_a}. \tag{11}$$

In the surface of $r = r_c$, it should have

$$\left.\begin{aligned}E_\theta &= \Delta_{\mathrm{i}} Z_0 H_\varphi\\ E_\varphi &= -\Delta_{\mathrm{i}} Z_0 H_\theta\end{aligned}\right|_{r=r_c}. \tag{12}$$

In Eqs. (11) and (12) the sign is different due to that the plus direction of r departs from the ground, and points to the ionosphere.

Through placing Eq. (10) to Eqs. (1), (2) and (3), the following component expressions in the wave guide may be obtained:

$$E_r = \frac{-Z_0 k^2 I\mathrm{d}l}{4\pi v_b^2 v^2}\begin{cases}\sum\limits_{n=0}^{\infty}n(n+1)(2n+1)[c_n H_n(v)+(H_n(v_b)+b_n)j_n(v)]P_n(\cos\theta), & v<v_b\\ \sum\limits_{n=0}^{\infty}n(n+1)(2n+1)[b_n j_n(v)+H_n(v)(c_n+j_n(v_b))]P_n(\cos\theta), & v>v_b\end{cases}, \tag{13}$$

$$E_\theta = \frac{Z_0 k^2 I\mathrm{d}l}{4\pi v_b^2 v}\begin{cases}\sum\limits_{n=0}^{\infty}(2n+1)\left[c_n H_n'(v)+(H_n(v_b)+b_n)j_n'(v)\right]P_n^1(\cos\theta), & v<v_b\\ \sum\limits_{n=0}^{\infty}(2n+1)\left[b_n j_n'(v)+(j_n(v_b)+c_n)H_n'(v)\right]P_n^1(\cos\theta), & v>v_b\end{cases}, \tag{14}$$

$$H_\varphi = \frac{\mathrm{i}k^2 I\mathrm{d}l}{4\pi v_b^2 v}\begin{cases}\sum\limits_{n=0}^{\infty}(2n+1)[c_n H_n(v)+(H_n(v_b)+b_n)j_n(v)]P_n^1(\cos\theta), & v<v_b\\ \sum\limits_{n=0}^{\infty}(2n+1)[b_n j_n(v)+(j_n(v_b)+c_n)H_n(v)]P_n^1(\cos\theta), & v>v_b\end{cases}. \tag{15}$$

In the surface of $r = r_a$ and $r = r_c$, each tangent direction component of the electromagnetic field should satisfy the impedance boundary condition in Eqs. (11) and (12). Therefore the following equations may be derived:

$$(H_n(v_b)+b_n)j_n'(v_a)+c_n H_n'(v_a) = -\mathrm{i}\Delta_g[(H_n(v_b)+b_n)j_n(v_a)+c_n H_n(v_a)], \tag{16}$$

and

$$b_n j_n'(v_c)+(j_n(v_b)+c_n)H_n'(v_c) = \mathrm{i}\Delta_{\mathrm{i}}[b_n j_n(v_c)+(j_n(v_b)+c_n)H_n(v_c)]. \tag{17}$$

From Eqs. (16) and (17) the coefficient b_n and c_n may be solved as:

$$b_n = \frac{\left\{H_n(v_b)\left[\mathrm{i}\Delta_\mathrm{i}H_n(v_c)-H_n'(v_c)\right]\left[\mathrm{i}\Delta_\mathrm{g}j_n(v_a)+j_n'(v_a)\right]-\left[\mathrm{i}\Delta_\mathrm{g}H_n(v_a)+H_n'(v_a)\right]\left[\mathrm{i}\Delta_\mathrm{i}H_n(v_c)-H_n'(v_c)\right]j_n(v_b)\right\}}{\left\{\left[\mathrm{i}\Delta_\mathrm{i}j_n(v_c)-j_n'(v_c)\right]\left[\mathrm{i}\Delta_\mathrm{g}H_n(v_a)+H_n'(v_a)\right]+\left[\mathrm{i}\Delta_\mathrm{g}j_n(v_a)+j_n'(v_a)\right]\left[H_n'(v_c)-\mathrm{i}\Delta_\mathrm{i}H_n(v_c)\right]\right\}}, \tag{18}$$

$$c_n = \frac{\left\{j_n(v_b)\left[\mathrm{i}\Delta_\mathrm{i}H_n(v_c)-H_n'(v_c)\right]\left[\mathrm{i}\Delta_\mathrm{g}j_n(v_a)+j_n'(v_a)\right]-\left[\mathrm{i}\Delta_\mathrm{i}j_n(v_c)-j_n'(v_c)\right]\left[j_n'(v_a)+\mathrm{i}\Delta_\mathrm{g}j_n(v_a)\right]H_n(v_b)\right\}}{\left\{\left[\mathrm{i}\Delta_\mathrm{i}j_n(v_c)-j_n'(v_c)\right]\left[\mathrm{i}\Delta_\mathrm{g}H_n(v_a)+H_n'(v_a)\right]+\left[\mathrm{i}\Delta_\mathrm{g}j_n(v_a)+j_n'(v_a)\right]\left[H_n'(v_c)-\mathrm{i}\Delta_\mathrm{i}H_n(v_c)\right]\right\}}. \tag{19}$$

3 Speeding numerical convergence algorithm of the field component

Placing Eqs. (18) and (19) into Eqs. (13), (14) and (15), each electromagnetic field expression between the ground and the ionosphere can be obtained, and all these series are absolutely convergent. But the velocity of their convergence is very low and it is difficult to obtain the satisfactory calculation precision with the direct summation method. In order to correctly determine the space variation [9] of the electromagnetic field, we must use a method which can improve the convergence. First, we looked at whether we can obtain the sum of the series when the ground and the ionosphere are both ideal electric conductors.

When $\Delta_\mathrm{g} = \Delta_\mathrm{i} = 0$, the coefficients b_n and c_n respectively degenerate as

$$b_n^0 = -\frac{j_n'(v_a)H_n(v_b)H_n'(v_c)-j_n(v_b)H_n'(v_a)H_n'(v_c)}{j'(v_a)H_n'(v_c)-j'(v_c)H_n'(v_a)}, \tag{20}$$

$$c_n^0 = -\frac{j_n'(v_a)j_n(v_b)H_n'(v_c)-j_n'(v_a)j_n'(v_c)H_n(v_b)}{j_n'(v_a)H_n'(v_c)-j_n'(v_c)H_n'(v_a)}. \tag{21}$$

When $n \gg v$, by the series expression of the circular cylinder function near the zero point, we achieve

$$(2n+1)H_n(v_b)j_n(v_a) \underset{n\to\infty}{\to} -\mathrm{i}\rho^{n+1}v_b, \tag{22}$$

where $\rho = \dfrac{r_a}{r_b} = \dfrac{v_a}{v_b}$, and

$$T_n = (2n+1)\left[b_n^0 j_n(v_a)+c_n^0 H_n(v_a)\right] \overset{n\to\infty}{\Rightarrow} -\frac{\mathrm{i}v_b}{n(n+1)} \times \left[(n+1)^2\rho^{n+1}+(2n+1)\times\left(n\rho^{-n}+(n+1)\rho^{n+1}\right)\sum_{m=1}^{20}\tau^{m(2n+1)}\right], \tag{23}$$

where $\tau = v_a/v_c$.

Up to now, we have obtained the general term's approximation of the series in the situation of the ideal electric conductor,

$$E_{rn} \underset{n\to\infty}{\to} \tilde{E}_{rn} = \frac{\mathrm{i}Z_0k^2Idl}{4\pi v_b v_a^2}\left[(n+1)(2n+1)\rho^{n+1}+(2n+1)\left(n\rho^{-n}+(n+1)\rho^{n+1}\right)\sum_{m=1}^{20}\tau^{m(2n+1)}\right]. \tag{24}$$

Consider the following sums of the infinite series:

$$\sum_{n=0}^{\infty}\tau^n P_n(x) = \frac{1}{g}, \tag{25}$$

$$\sum_{n=0}^{\infty}n\tau^n P_n(x) = \frac{\tau(x-\tau)}{g^3}, \tag{26}$$

$$\sum_{n=0}^{\infty}n^2\tau^n P_n(x) = \frac{\tau(x+x^2\tau-x\tau^2-2\tau+\tau^3)}{g^5}, \tag{27}$$

where

$$x = \cos\theta,\ \ g = \sqrt{1-2x\tau+\tau^2}.$$

Then,

$$\begin{aligned}\tilde{E}_r &= \sum_{n=0}^{\infty} \tilde{E}_{rn} P_n(\cos\theta) \\ &= \frac{\mathrm{i}Z_0 k^2 I \mathrm{d}l}{4\pi v_b v_a^2}\left[2\rho\frac{\tau_1\left(x+x^2\tau_1-x\tau_1^2-2\tau_1+\tau_1^3\right)}{g_1^5}\right. \\ &\quad \left. +3\rho\frac{\tau_1(x-\tau_1)}{g_1^3}+\rho\frac{1}{g_1}+M\right], \end{aligned} \tag{28}$$

where

$$\begin{aligned} M = \sum_{m=1}^{20}\left\{\tau^m\left[\frac{2\tau_2\left(x+x^2\tau_2-x\tau_2^2-2\tau_2+\tau_2^3\right)}{g_2^5}\right.\right. \\ +\frac{\tau_2(x-\tau_2)}{g_2^3}+2\rho\frac{\tau_3\left(x+x^2\tau_3-x\tau_3^2-2\tau_3+\tau_3^3\right)}{g_3^5} \\ \left.\left.+3\rho\frac{\tau_3(x-\tau_3)}{g_3^3}+\frac{\rho}{g_3}\right]\right\}, \end{aligned} \tag{29}$$

$$\tau_1=\rho,\ g_1=\sqrt{1-2x\tau_1+\tau_1^2},\ \tau_2=\frac{\tau^{2m}}{\rho},\ g_2=\sqrt{1-2x\tau_2+\tau_2^2},$$

$$\tau_3=\rho\tau^{2m},\ g_3=\sqrt{1-2x\tau_3+\tau_3^2}.$$

The right of Eq. (28) is an analysis expression which is easy to calculate and does not need to be summed term by term. Therefore we may rewrite Eq. (13) as

$$\begin{aligned} E_r &= \sum_{n=0}^{\infty} E_{rn} P_n(\cos\theta) \\ &= \sum_{n=0}^{\infty}\left(E_{rn}-\tilde{E}_{rn}\right)P_n(\cos\theta) \\ &\quad +\sum_{n=0}^{\infty}\tilde{E}_{rn}P_n(\cos\theta). \end{aligned} \tag{30}$$

Since the latter item in Eq. (30) can be derived by Eq. (28), while the amplitude of $\left(E_{rn}-\tilde{E}_{rn}\right)$ in the first term rapidly reduces with the increase of n, the series will rapidly converge and as a result the field will be calculated easily with better calculation precision.

At the SLF and ELF frequency band, the normalized surface impedance Δ_g and Δ_i of the ground and the ionosphere are very small. In the situation of the non-ideal electric conductor, if the series of E_r in Eq. (13) is rewritten similar to the series of Eq. (30), the first item is still small when n is very large and it can also speed up the numerical convergence velocity.

4 The algorithm of $P_n(v)$, $j_n(v)$ and $H_n(v)$

To calculate the first series of Eq. (30), we must specifically figure out the value of $P_n(v)$, $j_n(v)$ and $H_n(v)$. It is worth noting that when n is large, $j_n(v)$ is very small, and even tends to be zero, while $H_n(v)$ is very large, and tends to reach up to infinity, and both of them have exceeded the computer's precision. However, it should be noted that their product is still within the computer's precision. Therefore, we must calculate the product of $j_n(v)$ and $H_n(v)$. In this case, two kinds of situations of the low order and the high order should be derived.

When order n is small, the Bessel function needs to be calculated by the following recurrence formula:

$$\begin{aligned} &N_0(v)=-\cos v,\ N_1(v)=-\frac{\cos v}{v}-\sin v,\ j_0(v)=\sin v, \\ &N_{n+1}(v)=\frac{2n+1}{v}N_n(v)-N_{n-1}(v);\ j_1(v)=\frac{\sin v}{v}-\cos v, \\ &j_{n+1}(v)=\frac{2n+1}{v}j_n(v)-j_{n-1}(v);\ H_n(v)=j_n(v)+\mathrm{i}N_n(v); \\ &j_n'(v)=j_{n-1}(v)-\frac{n}{v}j_n(v);\ H_n'(v)=H_{n-1}(v)-\frac{n}{v}H_n(v). \end{aligned} \tag{31}$$

When n is large, the Bessel function needs to be calculated by the following formula with the mathematics handbook:

$$\begin{aligned} &f_n(v)=\frac{v}{n+\frac{1}{2}};\ S_n(v)=\sqrt{1-f_n^2(v)}; \\ &a_n(v)=\left(n+\frac{1}{2}\right)\{S_n(v)-\arctan h[S_n(v)]\}, \\ &j_n(v)\approx\left[\frac{1}{2}\sqrt{\frac{f_n(v)}{S_n(v)}}+\frac{1}{16}\left(\frac{f_n(v)}{S_n(v)}\right)^{\frac{3}{2}}v^{-1}\right. \\ &\qquad \left.-\frac{5}{48}\left(n+\frac{1}{2}\right)^2\left(\frac{f_n(v)}{S_n(v)}\right)^{\frac{7}{2}}v^{-3}\right]\mathrm{e}^{a_n(v)}, \\ &H_n(v)\approx-\mathrm{i}\left[\sqrt{\frac{f_n(v)}{S_n(v)}}-\frac{1}{8}\left(\frac{f_n(v)}{S_n(v)}\right)^{\frac{3}{2}}v^{-1}\right. \\ &\qquad \left.+\frac{5}{24}\left(n+\frac{1}{2}\right)^2\left(\frac{f_n(v)}{S_n(v)}\right)^{\frac{7}{2}}v^{-3}\right]\mathrm{e}^{-a_n(v)}. \end{aligned} \tag{32}$$

$P_n(v)$ can be calculated by the following iterative relation:

$$\begin{aligned} &P_0(x)=1,\ P_1(x)=x,\ P_2(x)=\frac{1}{2}\left(3x^2-1\right), \\ &P_{n+1}(x)=\frac{2n+1}{n+1}xP_n(x)-\frac{n}{n+1}P_{n-1}(x). \end{aligned} \tag{33}$$

According to the same method, H_φ and E_θ can be also figured out by employing the same speeding numerical convergence algorithm.

5 Calculation results and discussion

We have separately discussed two situations, that is, the non-ideal electric conductor condition ($\Delta_g = 0$, $\Delta_i \neq 0$) and the non-ideal electric conductor condition ($\Delta_g \neq 0$, $\Delta_i \neq 0$), and obtained the calculation results. In both cases, the height of the low ionosphere is taken as $h = 70$ km, the radius of the earth is $a = 6370$ km, the ground conductivity is $\sigma_g = 10^{-4}$, the ionosphere conductivity is $\sigma_i = 10^{-5}$ and the moment of the electric dipole is $Idl = 1$ Am.

Figure 2 shows the variation of the electric field component E_r along the propagation distance under the non-ideal electric conductor condition. The solid line is the calculated result of the spherical harmonic series speeding numerical convergence algorithm, which has been proposed in this paper. The dashed line represents the result of SLF second order spherical approximate formula proposed in Ref. [2]. Both the calculations are under the condition that the dipole and the receiving point are located on the ground, and the frequency is $f = 100$ Hz.

It may be seen from Fig. 2 that the two algorithms agree with each other quite well. Because the attenuation ratio of the SLF wave propagation in the wave guide is very small, we can clearly see that after 10000 km the speeding numerical convergence algorithm can correctly show the "interference" phenomenon of two waves propagating along the short great-circle way and the long great-circle way when it passes through the antipode to the receiver. However, the second order spherical approximate algorithm does not display this interference near the antipode. According to many propagation experiments on the SLF frequency band, it can be confirmed that the second order spherical approximate algorithm can correctly demonstrate the propagation rule of the SLF wave except when it is near the antipode. Therefore, the speeding numerical convergence algorithm of this paper is correct and it may be extended to the ELF frequency band.

Figure 3 shows the variation of three different frequency electromagnetic fields along the propagation distance under the non-ideal electric conductor condition, which is calculated by the speeding numerical convergence algorithm. The calculation condition requires the dipole and the receiving point be located on the ground, and the frequencies are $f = 1$ Hz, $f = 10$ Hz and $f = 100$ Hz, respectively.

Assuming $f = 100$ Hz and taking into account the absorption loss of the ground or the ionosphere, it can be seen from Fig. 3 that the electromagnetic field in the wave guide is a "traveling wave", which can also be taken as the sum of two "traveling waves" with the short great-circle way and the long great-circle way under the dissipative condition. Nonetheless, at the frequencies of $f = 1$ Hz and $f = 10$ Hz, because the length of the wave and the perimeter of the earth are comparable, the fields between the ground and the ionosphere are "standing wave".

Figure 4 shows the variation of the electric field component E_r along the height under the non-ideal conductor condition, where the solid line represents the result calculated by the speeding numerical convergence algorithm, and the dashed line represents the result obtained by the SLF spherical surface second order approximate algorithm. The calculation condition specifies that the dipole be located on the ground, while the receiving point should be located between the ground and the ionosphere, and the frequency should be $f = 100$ Hz, $\theta = \pi/3$.

From Fig. 4, it can be observed that the results of the two algorithms are similar to each other, and their difference is less than 0.2 dB. When the height increases,

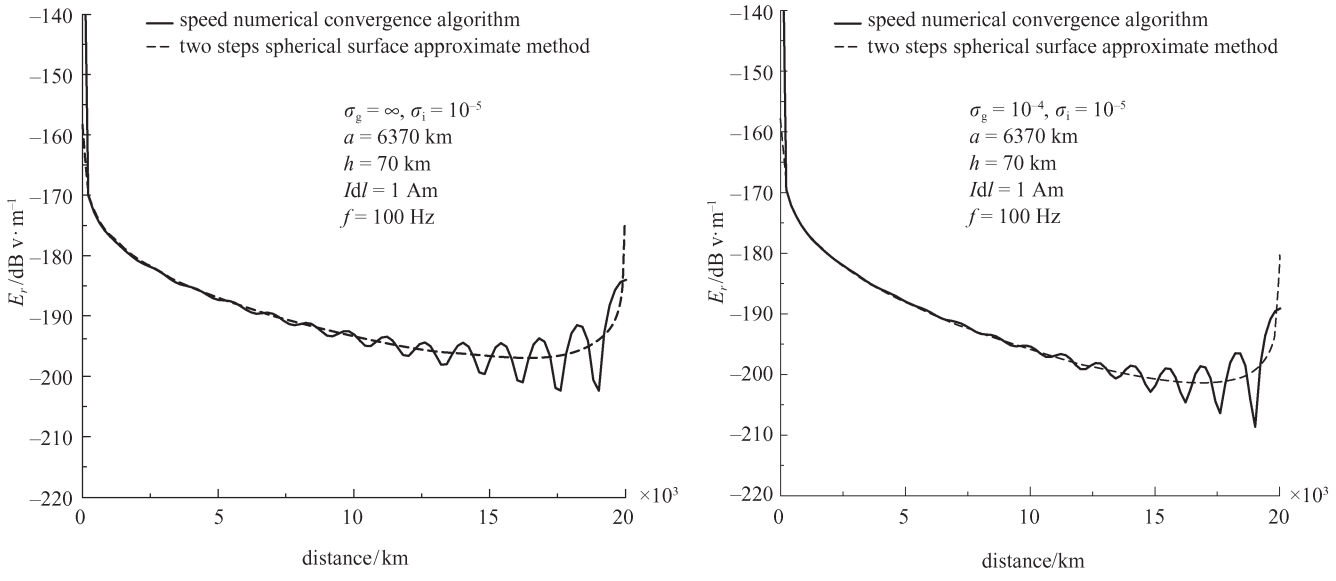

Fig. 2 Variation of the electric field component E_r excited by vertical electric dipole in earth-ionosphere cavity along the propagation distance

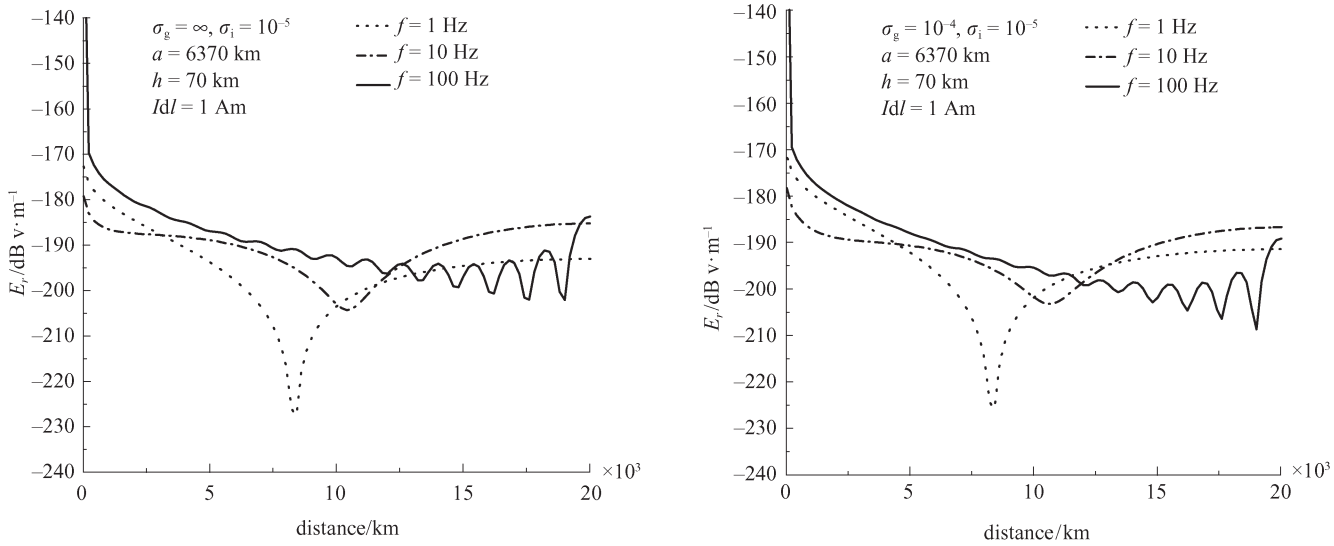

Fig. 3 Variation of the electric field component E_r excited by vertical electric dipole in earth-ionosphere cavity along the propagation distance

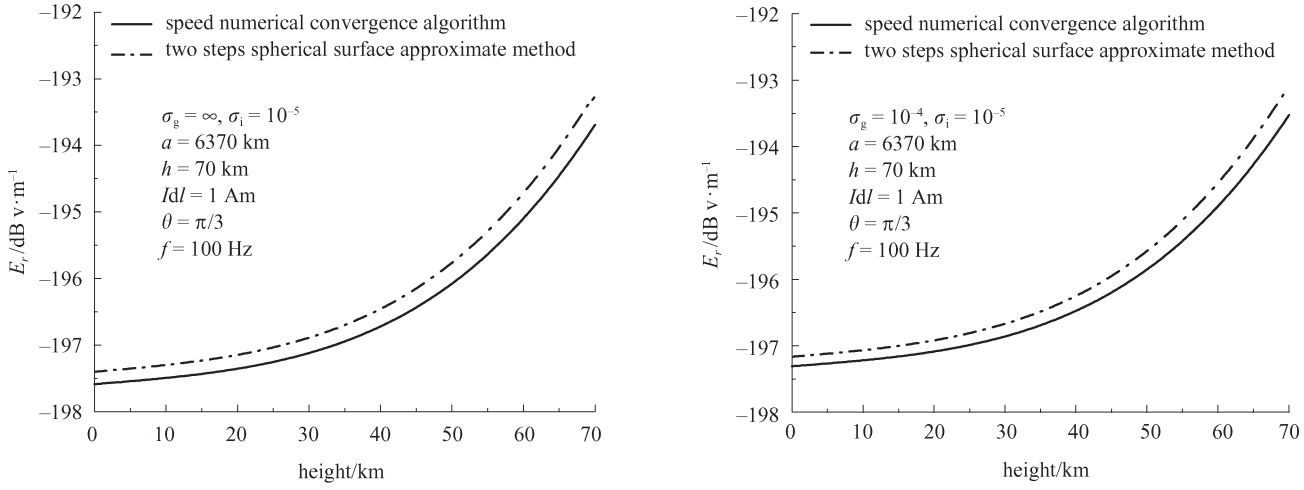

Fig. 4 Variation of the electric field component E_r excited by vertical electric dipole in earth-ionosphere cavity along height

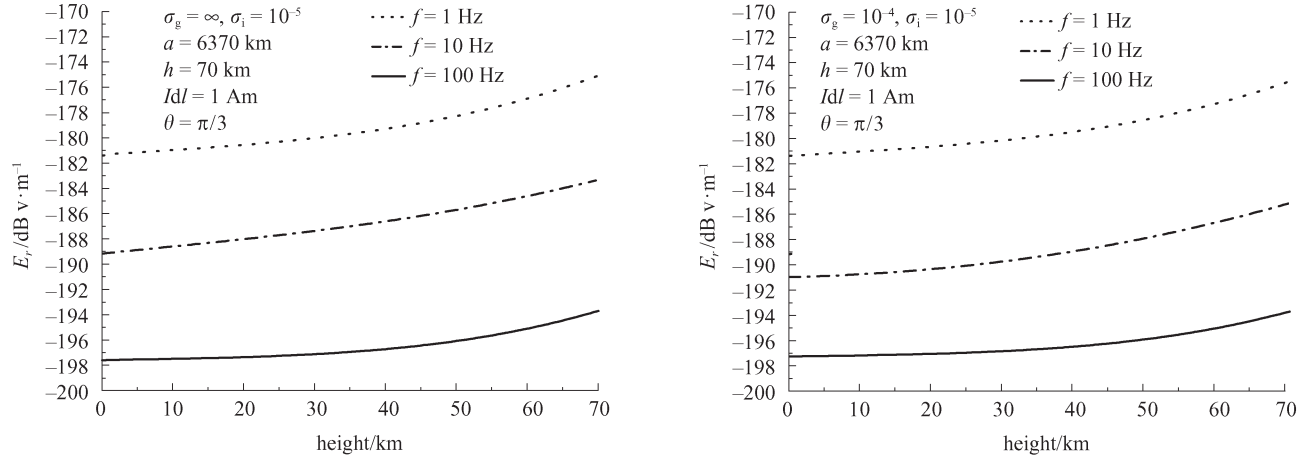

Fig. 5 Variation of the electric field component E_r excited by vertical electric dipole in earth-ionosphere cavity along height

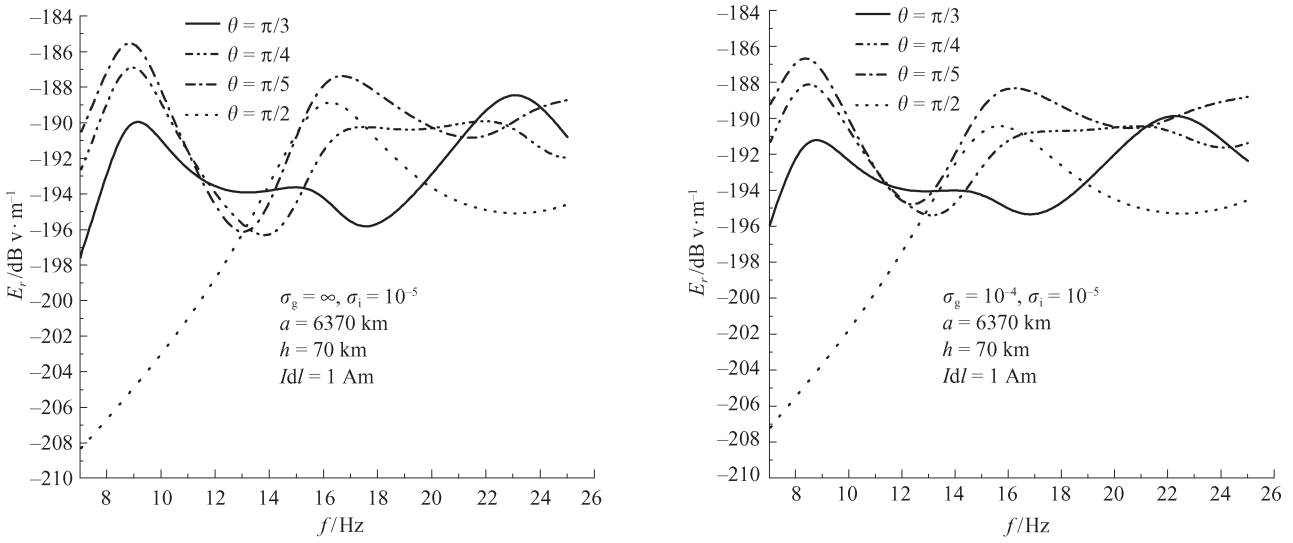

Fig. 6 Variation of the electric field component E_r excited by vertical electric dipole in earth-ionosphere cavity with frequency

the electric field component E_r increases slowly, and its amplitude variation is not very significant.

Figure 5 shows the variation of the electric field component E_r excited by the vertical electric dipole at several different frequencies along the height under the non-ideal conductor condition. It is calculated when the dipole locates at the ground, the receiving point locates between the ground and the ionosphere, and the frequency is $f = 1$ Hz, $f = 10$ Hz and $f = 100$ Hz, $\theta = \pi/3$ respectively.

It is demonstrated in Fig. 5 that as the height increases, the electric field component E_r increases gradually, and its amplitude variation does not increase significantly either.

Figure 6 shows the variation of the electric field component E_r with the frequency under the non-ideal conductor condition. It is calculated when both the receiving point and the dipole are located on the ground, and $\theta = \pi/3$, $\theta = \pi/4$, $\theta = \pi/5$ and $\theta = \pi/2$ respectively.

Compared with Fig. 7, Fig. 6 indicates that the resonance frequency is approximate to $f = 8.8$ Hz, $f = 16.5$ Hz and $f = 22.8$ Hz under the non-ideal electric conductor condition. Moreover, the resonance curve is smooth due to the absorption loss.

In Ref. [2], this kind of resonance phenomenon is called as Schumann's resonance, which has been validated by

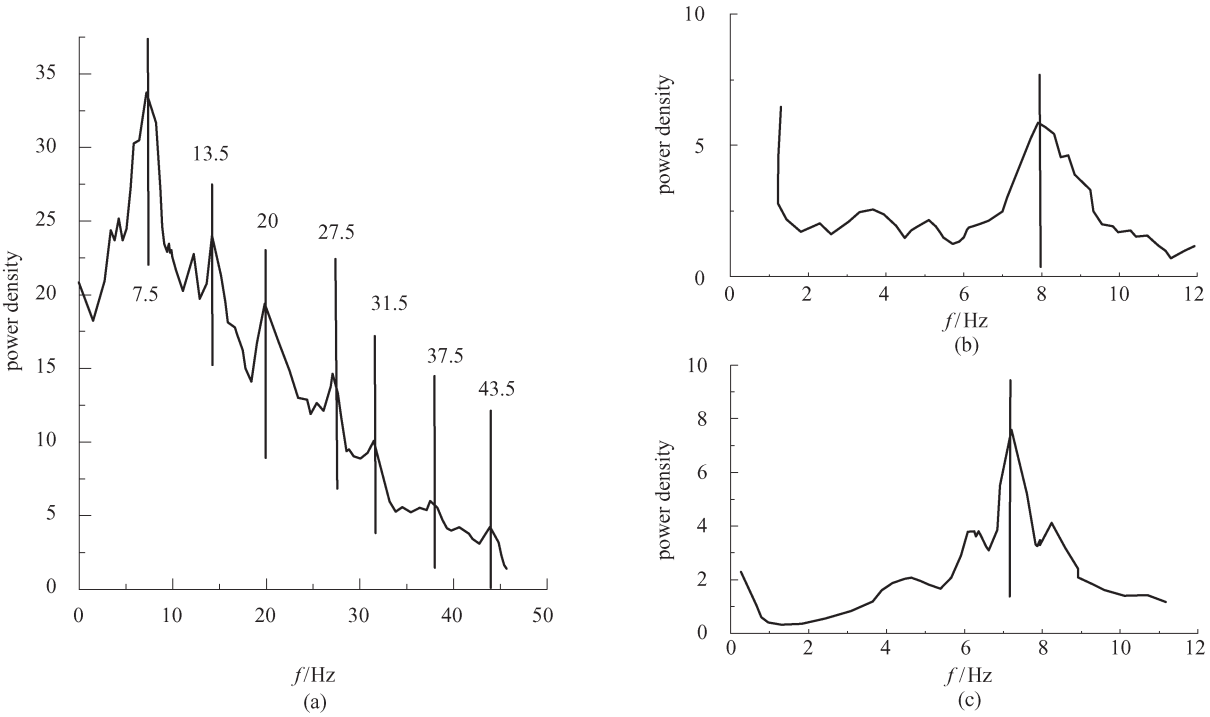

Fig. 7 Noise power spectrum which Larsen and Egeland measured in 1968

Larsen and Egeland in 1968. In Fig. 7, (a) was obtained by the record of 30 seconds, while (b) and (c) were obtained by the record of two minutes. Thus, it can be clearly seen that there is a ''resonance'' phenomenon near $f = 7.5$ Hz, $f = 14.5$ Hz and $f = 20.5$ Hz, which conforms to the calculation results.

6 Conclusions

A theoretical calculation of the VLF/SLF electric wave propagating among the earth-ionosphere wave guide generally utilizes the full wave method to solve the model equation. The field in the wave guide is comprehended as the sum of each wave mode. However, this method is very complex, and unsuitable to the ELF frequency band. In 1999 Barrick proposed that the field in the wave guide might be expanded to the spherical harmonic series based on Wait's [10] algorithm. Barrick directly calculated the electromagnetic field in the wave guide by using a type of speeding numerical convergence method, which is suitable for SLF/ELF frequency band. We have further developed Barrick's method and discussed two kinds of typical situations. Calculation results coincide with the known SLF correct results as well as the Schumann's resonance phenomenon in the ELF frequency band.

References

1. Tripathi V K, Chang C L, Papadopoulos K. Excitation of the Earth-ionosphere waveguide by an ELF source in the ionosphere. Radio Science, 1982, 17(5): 1321–1326
2. Galejs J. Stable solutions of ionospheric fields in the propagation of ELF and VLF waves. Radio Science, 1972, 7(5): 549–561
3. Pan W Y. Long Wave Beyond Long Wave Extremely Long Wave Propagation. Chengdu: Electric Scientific and Technical University Press, 2004 (in Chinese)
4. Shan X J. Earthquake electromagnetism satellite material assembly. Chinese Earthquake Bureau Research Institute of Geology, 2006 (in Chinese)
5. Galejs J. Terrestrial Propagation of Long Electromagnetic Wave. Pergamon Press, 1972
6. Zhang H Q, Pan W Y. The electromagnetic field of a vertical electric dipole over a spherical conductor covered by a dielectric layer. Chinese Journal of Radio Science, 2002, 17(4): 344–349 (in Chinese)
7. Zhu X Q, Pan W Y, Guan B R. Electromagnetic field produced by a vertical electric dipole on a negative-index media half space. Chinese Journal of Radio Science, 2006, 21(2): 177–183 (in Chinese)
8. Barrick D E. Exact ULF/ELF dipole field strengths in the Earth-ionosphere cavity over the Schumann resonance region: Idealized boundaries. Radio Science, 1999, 34(1): 209–227
9. Jeffrey A. Table of Integrals, Series and Products. NY: Academic Press, 1980
10. Wait J R. Electromagnetic Waves in Stratified Media. NY: Pergamon Tarrytown, 1962, 372